COATING PROCESS OF PHOTOSENSITIVE CYLINDERS

Danmer Maza Quinones
Department of Mechanical Engineering
Pontifical Catholic University of Rio de Janeiro – PUC-Rio
Rua Marquês de São Vicente 225, Gávea, Rio de Janeiro, Brasil
danmerm@mec.puc-rio.br

Márcio da Silveira Carvalho
Department of Mechanical Engineering
Pontifical Catholic University of Rio de Janeiro – PUC-Rio
Rua Marquês de São Vicente 225, Gávea, Rio de Janeiro, Brasil
msc@mec.puc-rio.br

Satish Kumar
Department of Chemical Engineering/Mat Sci
University of Minnesota
421 Washington Ave S E Minneapolis, MN 55455, USA
kumar030@umn.edu

Abstract. *Photosensitive cylinders are used in printing arts and more particularly in electrophotographic printing (xerographic copy). The photosensitive coating is applied to the cylinder in liquid form, before it is solidified. The liquid is applied to the cylinder through a needle applicator that translates along the direction of the cylinder axis. The cylinder rotates during this process in order to cover the entire surface. Therefore, the liquid is applied in a spiral pattern. To help spread liquid over the cylinder surface and improve the thickness uniformity, each liquid stream applied from the needle passes under a flexible blade. This process leads to a coating that presents a spiral pattern on the deposited layer thickness, that can cause defects on the electrophotographic process. The complete understanding of the flow is vital to the optimization of the process.*
A theoretical model of the thin film flow over the surface of a rotating cylinder is presented here. It is based on the lubrication approximation considering a thin precursor film in front of the apparent contact line. The resulting non-linear fourth-order PDE for the film thickness was solved by second-order finite difference method. The time discretization was done by using implicit Crank-Nicholson scheme. The non-linear algebraic equation at each time step was solved by Newton's method. The results show how the uniformity of the deposited layer varies with process parameters and liquid properties.

Keywords*: Liquid thin film, contact line, free boundary problem, finite difference methods*

1. INTRODUCTION

Photosensitive cylinders are used in the printing art and more particularly in Electrophotographic Printing (xerographic copy). The coating is applied to the cylinder by rotating it about its longitudinal axis and applying the liquid from an applicator in a spiral pattern. Then, the deposited layer is spread by using of a flexible blade as shown in Fig.1. This Process may lead to a non-uniform thickness profile on the roll surface if the operating parameters are not properly chosen. As in many other coating applications, the challenge in this process is to obtain a uniform liquid layer thickness.

The goal of this research is to develop a theoretical model in order to better understand how the different parameters affect the uniformity of the liquid layer that is deposited on photosensitive cylinders by the process described above.

The three dimensions, transient liquid flow is modeling using lubrication approximation and the appropriate boundary condition at liquid-air interface. The Navier-Stokes equation are simplified into a fourth-order partial differential equation that describe the liquid layer thickness varies with time and position.

Here, we report on the first two steps in the development of this complex theoretical model. First, the thin film flow over an inclined plane with two feed ports is analyzed. The goal is to study how two liquid drops originated from the feed ports merges and flow down the plane. The second step corresponds to the one-dimensional analysis of a thin film over a rotating cylinder. The goal is to study how the viscous drag from the roll rotation, surface tension forces and gravitational forces affects the thickness profile along the azimuthal direction. The last step, not reported here, is the combination of the two previous one, and will correspond to the complete two-dimensional thin film flows over a rotating cylinder with a moving feed port.

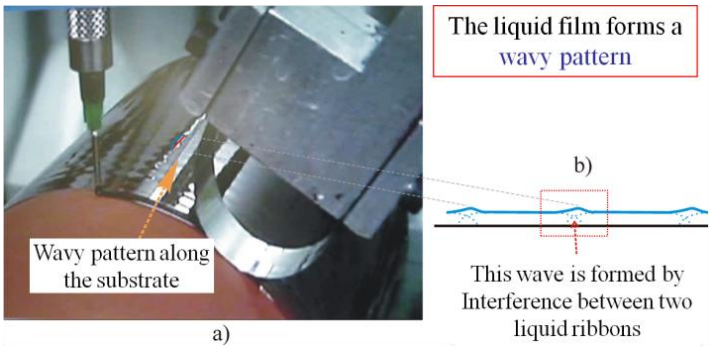

Figure 1. Coating process of photosensitive cylinder.

2. TWO-DIMENSIONAL FILM FLOW OVER AND INCLINED PLANE WITH FEED PORTS

The coating flow develops as a balance between viscous, surface tension forces and a body force. The body force is may be represented by gravity, centrifugal, or thermo-capillary force. Coating flows exhibit two main features: One is the existence of a free surface, whose position is unknown a priori, and the other one is the presence of a contact line, which defines the boundary between the film (main part-bulk) and the uncoated surface. The combination of these two features may lead to complex topologies of stable or unstable flows, with nontrivial shapes of the free surface and corrugations of the contact line.

2.1. Mathematical Formulation

The configuration of the thin film flow down a plane tilted at an angle α to the horizontal with two feed ports is sketched in Fig. 2. The coordinates system is chosen such that the *x*-axis is parallel to the plane, pointing in the downhill direction and *y*-axis is perpendicular direction on the plane. The height of the liquid layer *h(x,y,t)* is measured normal to the inclined plane.

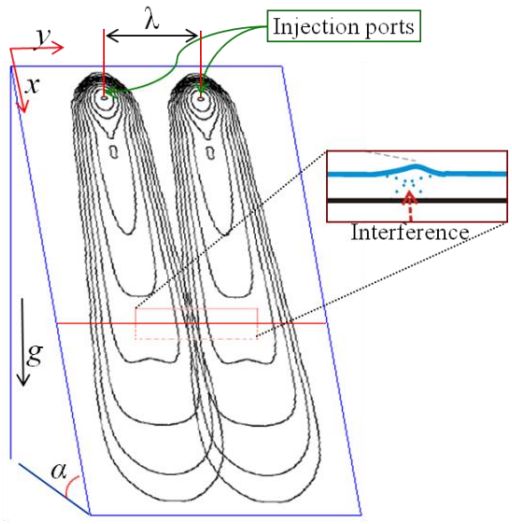

Figure 2. Sketch flow down an inclined plane with injection ports.

The Navier-Stokes equations with the appropriate boundary conditions at the liquid-air interface may be simplified using lubrication approximation, leading to the thin film flow equation:

$$\frac{\partial h}{\partial t} = -\frac{1}{3\mu}\nabla \cdot [\sigma h^3 \nabla \nabla^2 h - \rho g h^3 \nabla h \cos\alpha + \rho g h^3 \sin\alpha \, \boldsymbol{i}] + \mathcal{W}_j(x,y) \quad (1)$$

Where the μ is viscosity, σ is the surface tension and the g is the gravity. The three terms in Eq. (1) stand for the viscous, capillary, and gravitational forces, respectively. Here $\boldsymbol{i}$ is the unit vector along the *x*-axis, i.e. parallel to the inclined plane. This equation includes the nonslip boundary condition at the inclined plane surface. The liquid feed ports are adding an extra term to the equation that represents the liquid injection. Here $\mathcal{W}_j$ is the injection velocity

normal to the inclined plane (see Schwartz , 1988). Liquid is injected with a parabolic velocity profile through a circle of radius *R*, centered in the points (x_{cp1},y_{cp1}) and (x_{cp2},y_{cp2}). Thus,

$$\mathcal{W}_j = \begin{cases} \frac{2\Gamma}{\pi R^2}\left[1-(\frac{r}{R})^2\right]; & \text{for} \quad \left[\left(x-x_{cpj}\right)^2+\left(y-y_{cpj}\right)^2\right]^{1/2} \le R \\ 0\ ; & \text{for} \quad \left[\left(x-x_{cpj}\right)^2+\left(y-y_{cpj}\right)^2\right]^{1/2} > R \end{cases} \tag{2}$$

Γ is the volumetric feed rate and j={1,2}two feed ports.

Due to the well-known contact line paradox (macroscopic divergence of the viscous dissipation rate), theoretical and computational methods require some regularizing mechanism. There are two different approaches in the literature. One possibility is to relax the no-slip boundary condition at fluid–solid interface, introducing a slipping length l_s. The other approach, shown in fig. 3, is to assume the existence of a thin precursor film h_f ahead of apparent contact line.

Diez, Kondic and Bertozzi (2001), made an extensive comparison of these regularizing mechanisms. The main conclusion of these studies was that the precursor film model produced equivalent results to slip models when h_f=l_s. Because the computational performance of the precursor model is much better, we use this approach in this work. Typically, one chooses h_f to be one or two orders of magnitude smaller than the average bulk thickness. However, in order to be able to quantitatively reproduce experimental data, Diez et al. (2005) found that the precursor film thickness should be h_f=3x10^{-5}a; where a is the capillary length ($a = \sqrt{\sigma/\rho g}$). They found that the results are fully converged for a mesh size of $\Delta x = 10^{-3}a$. They have also verified that this value of h_f remains unchanged as the time step Δt changes. It is important to notice that this h_f is in the range of the thicknesses measured and reported in literature for precursor films.

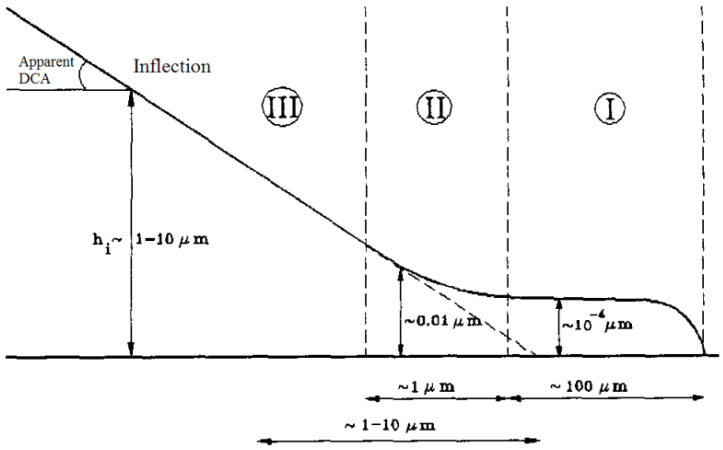

Figure 3. Schematic diagram of the different regions at the edge of the Drop extracted from Diez et al. (1994)

The boundary conditions used to integrate the fourth-order thin film equations are:

$$\frac{\partial h}{\partial x} = \frac{\partial^3 h}{\partial x^3} = 0, \quad \text{at} \quad x = 0, \qquad x = L_x \tag{3}$$

$$\frac{\partial h}{\partial y} = \frac{\partial^3 h}{\partial y^3} = 0, \quad \text{at} \quad y = 0, \qquad y = L_y \tag{4}$$

With the initial condition $h(x, y, t = 0) = h_f = 0.01$

The equation 1 was solving by finite difference method. The domain, defined by the rectangle $0 \le x \le L_x$ and $0 \le y \le L_y$, was divided by $N=n_x$ x n_y nodes, uniformly spaced in each direction. Details of the discretization schemes tested are discussed next.

2.2. Spatial Discretization

The discretization used here is the second-order proposed by Diez and Kondic (2002). The discretization of the term corresponding to the capillary forces, i.e. $\nabla \cdot [\sigma h^3 \nabla \nabla^2 h]$, requires special attention. Because h represent a film

thickness, it is crucial that its value remains positive throughout the calculation. Because the precursor film thickness is very small and the derivatives near to the apparent contact line very high, discretization errors may lead to negative values of the film thickness. It is important to use a positive preserving scheme (PPS) in the finite difference discretization.

The approximation of each term of the film flow equation is given by:

$$\nabla \cdot [\sigma h^3 \nabla \nabla^2 h] \approx \sigma \nabla \cdot [D_k \nabla \nabla^2 h]$$

$$\nabla \cdot [\rho g h^3 \nabla h \cos \alpha] \approx \rho g \nabla \cdot [G_k \nabla h] \cos \alpha \quad (5)$$

$$\nabla \cdot [\rho g h^3 \sin \alpha \, \mathrm{i}] \approx \rho g \nabla \cdot [G_k \mathrm{i}] \sin \alpha$$

The PPS prescribes the following interpolation of the diffusivity term at the node k (h_k is defined at the center of the line element (x_i , x_{i+1})) leads to the following expression for D_k in x and y directions:

$$D_k^{(x)} = 2\frac{h_k^2 h_{k+1}^2}{h_k + h_{k+1}}, \qquad D_k^{(y)} = 2\frac{h_k^2 h_{k+n_x}^2}{h_k + h_{k+n_x}} \quad (6)$$

The Gravity terms were discretized using centered finite difference as:

$$G_k^{(x)} = \frac{h_k^3 + h_{k+1}^3}{2}, \qquad G_k^{(y)} = \frac{h_k^3 + h_{k+n_x}^3}{2} \quad (7)$$

2.3. The time Discretization

The time discretization is performed by a Crank-Nicholson scheme θ=1/2, (Implicid, $O(\Delta t^2)$)

$$\frac{h_k^{n+1} - h_k^n}{\Delta t^n} + \theta f_k^{n+1} + (1-\theta) f_k^n = 0 \quad (8)$$

This equation forms a system of N non linear algebraic equations, which are solved using Newton's method.
The Crank-Nicholson scheme leads to an unconditionally stable method. However, one still needs to consider a number of issues when deciding on the size of the time step. An important requirement is that the solution has to be strictly positive; too large of a time step may lead to negative film thickness (Diez and Kondic, 2002).

Because we are using Newton's method to solve the non-linear system at each step, it is important to have a good initial guess. A linear extrapolation of the two previous solution is used to calculate the initial guess and the time step is adjusted such that the number of Newton's step remains inside a given range. If, at given time step Newton's method converges in a small number of iterations, the time step for the next instant is doubled. On the other hand, if it takes too many steps, the time step is divided by two.

Since the Crank-Nicholson scheme is $O(\Delta t^2)$, the relative error of the numerical solution at the point k is given by:

$$E_k = \frac{(\Delta t^n)^2}{h_k^n} \left| \frac{d^2 h_k^n}{dt^2} \right| \quad (9)$$

Making the expansion around h_k^n and h_k^{n-1} by Δt^{n-1} and Δt^n (time steps performed before and after t^n), respectively, we obtain the maximum relative error:

$$E = \max_{1 \ll k \ll N} \left\{ \frac{2\Delta t^n}{\Delta t^{n-1}} \frac{[\Delta t^{n-1} h_k^{n+1} + \Delta t^n h_k^{n-1} - (\Delta t^{n-1} + \Delta t^n) h_k^n]}{(\Delta t^{n-1} + \Delta t^n)} \right\} \quad (10)$$

If E less than a given tolerance Tol(typically, Tol=10^{-2}-10^{-3}), the solution h^{k+1} obtained using time step Δt^k is accepted; otherwise, the time step is reduced and a new iteration is performed.

2.3. Results

The numerical code validation it was made using known analytical solution for pure spreading of a single drop on horizontal surfaces with and without injection. The drops spreading follows a power law $x_f \sim t^n$, where x_f is the front position, t the time and n the power law exponent. The first case, *without injection*, Ehrhard and Davis(1991) shown typically values for "n" according to the dominant force (ST and G denote surface-tension and gravity dominance, respectively). "Table 1" shows the values obtained numerically and analytically for this first case.

For the second case, with injection, Holdich et al. (2006) deducing analytically values of "*n*" for capillary and gravitational regimes for different flows rate. Those values are given in the Tab. 2.

Table 1. Comparison between analytical and numerical results for the power law exponent "n"

Ca	Numerical *n*	Theory *n*	Dominance force
0.002	0.11	0.1	ST
6.54	0.124	0.125	G

Table 2. Comparison between analytical and numerical results for "n" considering flow injection

Dominance force	Ca	Injection Flow Rate Γ (cm^3/s)	Numerical *n*	Theory *n*
ST	0.002	0.1	0.405	0.4
		1.0	0.407	
		10.0	0.407	
G	6.54	0.1	0.474	0.5
		1.0	0.485	
		10.0	0.489	

We can see good agreement with theoretically predicted exponents, but all of them are analyzed for a one single drop. There are no analytical solutions for problems involving interaction between two or more drops for inclined plane. More recently, coalescence of two mercury drops (Menchaca-Rocha et al, 2001) and water drops (Andrieu et al, 2002) on a horizontal solid surface was analyzed experimentally. However, in those works the fluid is strongly nonwetting, here is important to reveal we consider only completely wetting fluids. In this work we can compare just qualitative features of the results.

Simulations for inclined plane were performed for a Newtonian liquid with tension surface σ=19.8 dyn/cm, density ρ=0.96 g/cm^3, and kinematic viscosity υ=*20*St, so that the capillary length is $a = \sqrt{\sigma/\rho g} = 0.145cm$. Radio of the port injection R = 1mm.

Figure 4 shows the front position x_f for different angles α= 90º, 60º, 45º, 15º at the same feed rate $\Gamma = 0.1cm^3/s$, for each port and the same distance, λ=1.2cm, between them (see Fig. 2). When the plane is vertical, α= 90º, the gravitational forces are strong and the velocity of the front positions is the highest among the cases analyzed. The velocity down the plane is high enough that there is not lateral interaction between the two drops. At α= 60 º and 45º, the velocity of the front position decrease and for those configurations appears lateral interaction between the drops, but that interaction is not considerable to change his asymptotical behavior. An inflection point in the downward velocity plot can be observed when the drops merge. At α= 15º, the downward velocity is so small that the drops coalesce soon after flowing out of the feed ports and the liquid flow down the plane as a single drop.

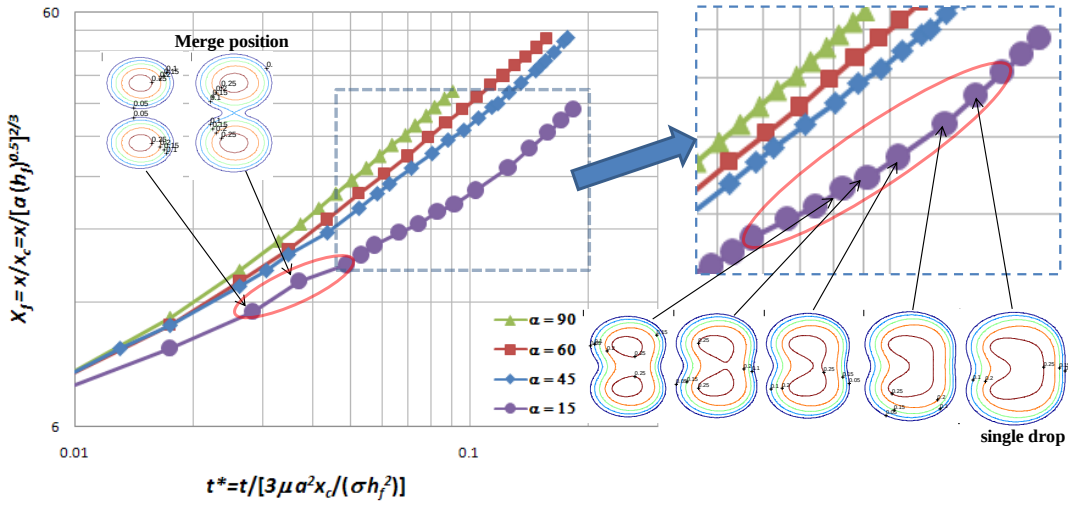

Figure 4. Front position at different α with the same feed rate Γ

3. ONE-DIMENSIONAL FILM FLOW OVER A ROTATIONAL CYLINDER

In this section, the one-dimensional thin film flow over a rotating cylinder is analyzed. The curvature of the surface and its movement are now included in the model. Rotation radically changes the coating, by preventing unlimited drainage to the underside. For sufficiently fast rotation, viscous forces alone are able to maintain a coating. However, at lower speeds, fluid drainage leads to the formation of drops on the cylinder underside. If these drops grow large enough, coating material may drip from the cylinder. At these speeds, and for a stationary cylinder, surface tension is clearly essential to retain coating on the cylinder.

The one-dimensional model presented in this section is validated by comparing the predictions to the limiting case of stationary cylinder, to Moffatt's solution (Moffatt, 1977), and to the recent work of Weidner et al. (1997) and Evans et al. (2004).

3.1 Mathematical Formulation

The model here is one-dimensional film thickness; variation along the cylinder axis is neglected. Figure 5 illustrate the situation and the coordinate system used. For the one-dimensional problem, the coating thickness h depends only on time t and azimuthal coordinate θ, $h = h(\theta, t)$. Throughout this section, the cylinder rotation rate Ω, and the coating viscosity μ, density ρ and surface tension σ, are all assumed constant.

Moffatt (1977) presented a theory that balanced cylinder rotation and gravitational drainage. In this case, the liquid flux at any point is given by:

$$\boldsymbol{Q(\theta) = R\Omega h - \frac{\rho g}{3\mu} h^3 \cos\theta} \tag{11}$$

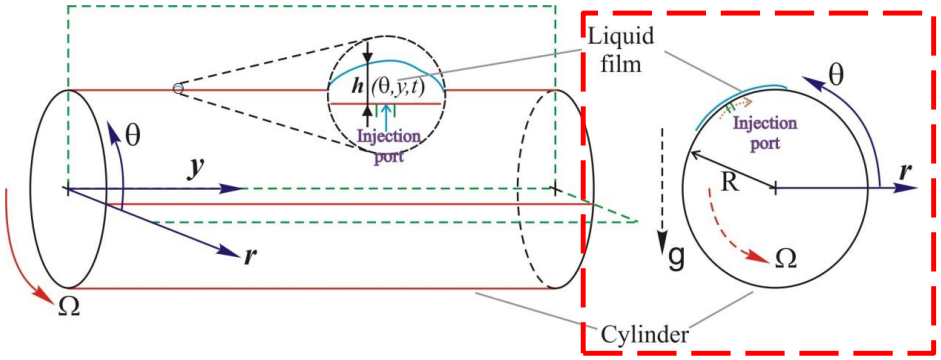

Figure 5. The rotating cylinder and its coordinate system.

where R is the cylinder radius, θ is measured as shown in Figure 6, and g is the gravitational acceleration. In steady state, the requirement that Q be uniform (independent of θ) gives a cubic equation for h. The thickest coating occurs at $\theta = 0$, where the flow due to rotation is most opposed by drainage. Moffatt found that for a coating on the outside of the cylinder, of mean thickness ho, this model allows no steady solutions for rotation rates less than a critical value Ω_c, given by:

$$\frac{\mu\Omega_c}{\rho g R} = \left(\frac{2\pi}{4.428}\right)^2 \left(\frac{h_o}{R}\right)^2 \tag{12}$$

The evolution equation for the film thickness h in cylindrical coordinate and considering the roll rotation is given by the following expression:

$$\frac{\partial h}{\partial t} + MW\frac{\partial h}{\partial \theta} - \frac{\partial}{\partial \theta}\left(\frac{h^3}{3}\cos\theta\right) + \nabla\cdot\left\{\frac{h^3}{3Bo}\nabla(h+\nabla^2 h) + \frac{h^3}{3}[W^2 - sin\,\theta]\nabla h\right\} = 0 \tag{13}$$

The behavior of the coating is determined by three parameters: M, W and Bo ($M = \frac{\mu}{\rho\sqrt{gR^3}}; W = \frac{\Omega}{\sqrt{g/R}}$).

Where Bo represents the Bound number, W^2 represent the dimensionless rotation rate and MW is the ratio of the wall speed $R\Omega$ to the velocity scale U ($U=\rho g H^2/\mu$), where H is the characteristic thin film thickness).

In 1D model the axial variation is ignored. And so, the evolution equation to be solved for $h(\theta,t)$ is therefore:

$$\boldsymbol{\frac{\partial h}{\partial t} + MW\frac{\partial h}{\partial \theta} - \frac{\partial}{\partial \theta}\left(\frac{h^3}{3}\cos\theta\right) + \frac{\partial}{\partial \theta}\left\{\frac{h^3}{3Bo}\frac{\partial}{\partial \theta}\left(h + \frac{\partial^2 h}{\partial \theta^2}\right) + \frac{h^3}{3}[W^2 - sin\,\theta]\frac{\partial h}{\partial \theta}\right\} = 0} \tag{14}$$

Periodic boundary condition is used:

$$h(\theta = 0\,, t) = h(\theta = 2\pi, t)$$

$$\frac{\partial h}{\partial \theta}(\theta = 0\,, t) = \frac{\partial h}{\partial \theta}(\theta = 2\pi, t)$$

3.2 Spatial Discretization

The domain is divided by n_θ uniformly spaced grid points ($\Delta\theta$=2π/n_θ). The capillary pressure term is again approximated by a PPS scheme. As in the previous section, Crank-Nicholson method was used to approximate the time derivative. The discrete version of the film flow equation-eq.(14)- at node *k* is given by:

$$\frac{\partial}{\partial \theta}\left\{h^3 \frac{\partial}{\partial \theta}\left(\frac{\partial^2 h}{\partial \theta^2}\right)\right\} \approx \frac{\partial}{\partial \theta}\left\{D_k \frac{\partial}{\partial \theta}\left(\frac{\partial^2 h}{\partial \theta^2}\right)\right\} \tag{15}$$

$$\frac{\partial}{\partial \theta}\left\{h^3 \frac{\partial h}{\partial \theta}\right\} \approx \frac{\partial}{\partial \theta}\left\{G_k \frac{\partial h}{\partial \theta}\right\} \tag{16}$$

$$\frac{\partial}{\partial \theta}(h^3 \cos\theta) \approx \frac{\partial}{\partial \theta}(G_k \cos\theta) \tag{17}$$

Where D_k and G_k were indicated in the previous section. for $\frac{\partial h}{\partial \theta}$ we use centered finite difference.

3.3. Results and validation (Stationary cylinder)

The free surface profile at the limiting case of stationary cylinder (*W*=0) can be obtained analytically. Weidner et al. (1997) considered the hypothetical situation of a static drop hanging beneath the cylinder; with no variation along the cylinder axis (see Figure 6). In reality, such a configuration would be unstable to perturbations along the cylinder axis. In the results presented here, 400 grid points were used along the circumference of the roll. Accuracy was verified by using more grid points and noting that the solutions did not change within the desired accuracy.

Figure 6 shows the validation of this one-dimensional model for a cylinder of radius *R*=10*a* and *h*(*t*=0)= 0.000737*R*. The coating profile from the static theory, using full curvature an approximate form (see Weidner, 1997) is in agreement with the numerical method proposed in this work. When the cylinder is stationary, a large drop forms on the underside of the cylinder into which liquid continues to drain even at very large times. The coating layer continually thins at the top $\theta=\pi/2$ reaching zero thickness asymptotically, and remains symmetric about a vertical axis at all times.

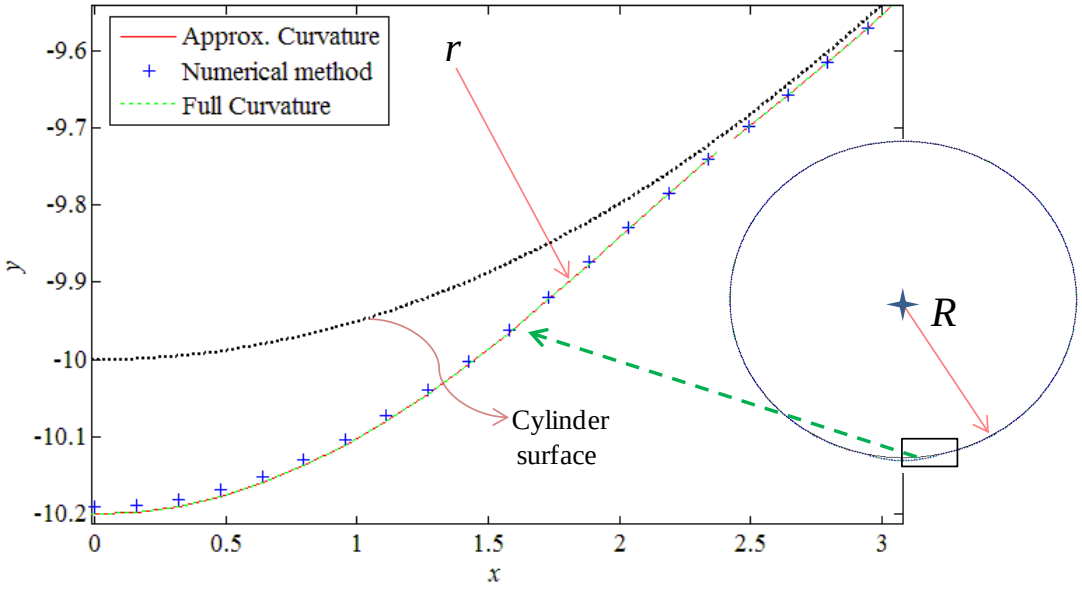

Figure 6. Numerical model compared to static drop shapes for a cylinder of radius *R*=10*a*. The shape of the static drop is computed using both the full curvature and an approximate form. The full and approximate curvature solutions are almost indistinguishable.

For non-stationary cylinder, simulations were performed for a cylinder with radius R=10a , Bo=100, rotating at various speeds. The liquid profile at the underside of roll at different roll speeds is shown in Fig.7. All simulations started with a layer of uniform thickness h_0=0.000737R and a viscosity parameter of M = 0.007. With these parameters, the critical speed of Eq. 14 corresponds to W=Wc=*0.0141*(associated to Ω_C).
When the cylinder is rotating, liquid is carried toward the upward-moving side of the cylinder, and vertical symmetry is lost. As W approaches W_c , the layer becomes more uniform, and the point of maximum layer thickness moves upward.

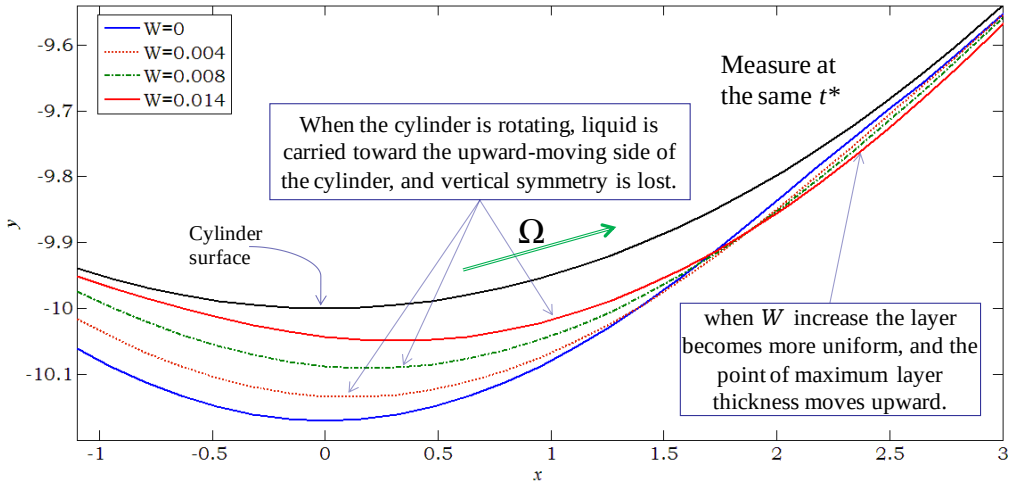

Figure 7. Final coating profiles for different W and considering for all the same M=0.007.

4. CONCLUSION

This paper discusses the fundamental problem of a liquid flow down a plane and over a rotating cylinder. These two problems were used as steps to the analysis of the coating process of photosensitive cylinders. The results show how the different liquid properties and process conditions affect the liquid profile.

5. REFERENCES

Andrieu, C., Beysens, D. A., Nikolayev, V. S., Pomeau,Y. 2002, "Coalescence of sessile drops" J. Fluid Mech, 453, 427-438

Bertozzi, A. L.,1998, "The mathematics of moving contact lines in thin liquid films", Notices Amer. Math. Soc., 45, pp. 689–697

Diez, J., Kondic, L. and Bertozzi, A. L., 2001, "Global models for moving contact lines", Phys. Rev. E, 63, pp. 011208.

Diez, J., Kondic, L.,2002, "Computing three-dimensional thin film flows including contact lines", J. Comp. Phys. 183 p.274

Diez, J., Gonzales, A.G., Gomba, J., Gratton, R. and Kondic, L., 2005, "Unstable spreading of a fluid filament on a vertical plane: Experiments and simulations", Phys. D, 209, 49-61.

Diez, J., Gratton, Thomas, L.P., Marino, B., 1994, "Laplace pressure-driven drop spreading: Quasi-self-similar solution", J. Colloid Interface 168, 15-20.

Ehrhard, P and Davis, SH., 1991, "Non-isothermal spreading of liquid drops on horizontal surfaces", J. Fluid Mech, 229, 365-388

Evans, P. L., Schwartz, L. W. and Roy, R. V.,2004, "Steady and unsteady solutions for coating flow on a rotating horizontal cylinder: Two-dimensional theoretical and numerical modeling", Phys. Vol. 16, 8.

Holdich, R., Starov, V.M., Prokopovich, P., Njobuenwu, D.O., Rubio, R.G., Zhdanov, S., Velarde, M.G., 2006 "Spreading of liquid drops from a liquid source", J. Colloid Interface 282, 247-255.

Menchaca-Rocha, A., Martinez-Davalos, A, Núnez, R., Popinet, S. and Zaleski, R., 2001, "Coalescence of liquid drops by surface tension", Phys. Rev. E 63, 046309

Moffatt, H. K., 1977, "Behavior of a viscous film on the outer surface of a rotating cylinder", J. Mec. 16, 651.

Schwartz, L. and Michaelides, E., 1988, "Gravity flow of a viscous liquid down a slope with injection", Letters.

Weidner, D. E., Schwartz, L. W. and Eres, M. H., 1997, ''Simulation of coating layer evolution and drop formation on horizontal cylinders,'' J. Colloid Interface Sci. 187, 243.

6. RESPONSIBILITY NOTICE

The authors are the only responsible for the printed material included in this paper.